PHYSIO - ELECTRICAL CHARACTERISTICS OF Sn/Pb SOLDER AFFECTED ALUMINUM SUBJECTED TO PLASTIC DEFORMATION AND THERMAL TREATMENT

Mohammad Salim Kaiser

Innovation Centre, International University of Business Agriculture and Technology Dhaka-1230, Bangladesh, dkaiser.res@iubat.edu

Received 07 March 2024
Accepted 22 November 2024
DOI: 10.59957/jctm.v60.i1.2025.13

ABSTRACT

In the present work, the precipitation behaviour of solder affected Al - Sn - Pb alloy is investigated as a function of cold deformation and artificial ageing using microhardness measurements, electrical resistivity, differential scanning calorimetry, X-Ray diffraction analysis as well as microstructural observation. To compare the aforementioned properties three different types of aluminium have been selected for analysis: commercially pure aluminium, binary aluminium with tin, and binary aluminium with lead. It has been found that changes in such parameters like cold rolling and thermal treatment play a crucial role in influencing the physio-electrical qualities of alloys. The alloys exhibit two distinct processes: solid solution strengthening combined with strain hardening resulting from cold plastic deformation, and the softening mechanisms of recovery and recrystallization. The presence of solder positively influences the hardness of pure aluminium at lower aging temperatures, primarily due to solid solution strengthening from tin and lead, albeit at the cost of conductivity. The superior performance of BCC tin over the similar FCC lead structure to Al is attributed to its unique crystal structure. Furthermore, neither of the two elements forms any intermetallic with Al, while Sn and cast alloy impurities do form a variety of intermetallic. DSC and XRD study also confirm the presence of those elements. The micrographs study of cold rolled alloys has confirmed elongated grain at the rolling direction and relatively thick grain boundaries of minor alloying elements due to the presence of different particles. All the alloys attain more or less re-crystallized state after ageing at 350ºC for one hour.

Keywords: Al - alloy, microstructure, resistivity, Sn - Pb solder, thermal ageing, work hardening.

INTRODUCTION

The primary good-conducting materials used widely include silver, copper, gold, and aluminium [1]. Among these materials, aluminium has emerged as the preferred choice in modern power transmission and distribution systems. This shift in preference towards aluminium is mainly attributed to its cost-effectiveness and lightweight properties when compared to copper, making it an increasingly popular option for various high-voltage applications. Because of aluminium's higher conductivity - to - weight ratio compare to copper, it is now used for wiring in buildings, aircraft, and appliances [2 - 4]. The cross section of an aluminium wire is 1.5 times greater than that of a copper wire, but it is two times lighter to pass the same current. Weight is a crucial factor in high-voltage power lines that transport electricity over long distances. Therefore, the primary overhead power lines solely utilize aluminium wires. Electrical and electronic components and wiring harnesses are increasing in weight due to additional functions such as vehicle safety and comfort. Soldering of Al plays a crucial role in creating precise electrical and thermal connections within confined spaces, serving to not only bond metals effectively but also to seal components securely. Its versatility is evident in a wide range of applications, from enhancing the performance of sensors and electronics to ensuring reliable power transmission through aluminium contacts and wire leads. Moreover, aluminium soldering stands out as an essential technique for sealing and maintaining aluminium heat exchangers, thereby contributing to the extended functionality and durability of various mechanisms and systems [5]. Aluminium is one of the most recyclable materials around the world today. During the process, it does not degrade material properties. Additionally, recycled aluminium requires only 5 % of the energy used to make primary aluminium and can have the similar properties as the parent metal [6, 7]. It is therefore an economically and environmentally effective metal to recycle. Pure Al does not offer the high strength being soft and ductile materials. It needs to develop properties for use in different sectors. The strength of aluminium alloys can be modified through various combinations of alloying, heat treating and cold working [8 - 10]. Different alloying elements have different crystal structures so the nature and level of variation of the properties must be varied. Sometimes alloys act in response due to heat treatment through strengthening. Different levels of heat treatment also affect different properties. Cold rolling is a process that plastically deforms materials employed to strengthen and harden them. The main disadvantage is earlier softening due to thermal effects. Alloying is done for many reasons, usually to increase strength, increase corrosion resistance, or reduce cost [8, 11, 12]. When one property increases, it can affect other properties. A large amount of data on the influence of alloying elements on aluminium can be found in the book published by S. Sivashankaranto [8]. Specifically, silicon lowers melting temperature and increases fluidity, while Cu provides strength and precipitation hardening, but reduces ductility and corrosion resistance. Mn improves work hardening but prevents stress corrosion cracking. Fe improves hardness but also reduces tensile properties in addition to corrosion.

The physical and electrical behaviour of aluminium under the influence of solder has been little studied by researchers in related fields such as the internet, libraries and other information sources. Moreover, implementation of plastic deformation along with thermal treatment is fully absents. In this study, the primary focus revolves around investigating the physico-electrical characteristics of solder-affected aluminium, particularly in relation to its response to work-hardening and heat treatment. To shed light on how specific alloying elements influence these properties, it conducted measurements on not only pure aluminium but also aluminium-tin and aluminium-lead alloys. This approach allows to discern and analyse the distinct impacts of these alloy combinations on the material's behaviour, contributing to a more comprehensive understanding of the subject matter. Successful completion will result in the correct determination of the optimal structure, processing parameters and properties of the current solder - affected aluminium scrap, which is expected to find a wider application, especially in industries with better properties; some possible applications include films, plates, heat exchanger stacks, exhaust bellows, hydraulic and pneumatic equipment, etc. Local production of such components from materials obtained through recycling processes significantly reduces the burden of importing goods from abroad.

EXPERIMENTAL

This study examines aluminium electrical wires and soldered connecting structures were considered after extensive use for several decades. For this purpose, waste aluminium wires are collected from multiple sources subjected to melting in a resistance furnace with the appropriate flux cover and the respective chemical compositions were examined. It was experiential that the resulting aluminium alloy contained a little percentage of tin and lead, with concentrations of approximately 1.43 and 1.20 weight percentages respectively. Simultaneously, three additional samples of commercially pure aluminium (99.75 %), along with Al - 1.51 wt. % Sn and Al - 1.28 wt. % Pb, were chosen to assess the impact of the two distinct soldering elements. The mould size was 300 x 150 x 20 mm. It was then subjected to a homogenization process at 450°C for 12 h, after which it was solutionized at 530°C for 2 h. The chemical composition of four alloys was analysed using Emission Spectroscopy and getting results are listed in Table 1. Cold rolling of solutionized alloys at 20, 40, 60 and 80 % were carried out using a 7.5 kW capacity laboratory scale rolling mill. For this cold rolling operation, the sample sizes were machined to the following dimensions: 15 x 16 x 300 mm, 7.5 x 16 x 300 mm, 5 x 16 x 300 mm and 3.75 x 16 x 300 mm. The samples were subsequently subjected to cold rolling, achieving final thicknesses of 3mm, specifically at 15, 7.5, 5, and 3.75 mm, resulting in a deformation of approximately 1.0 mm for each pass. Cast specimens were recognized as 0 % cold rolling. Samples that cold rolled were placed into isochronal and isothermal aging conditions, varying the temperature and duration accordingly. The hardness of various cold-rolled and heat-treated alloys was measured using a digital micro - vickers hardness tester model HVS - 1000Z at a load of 1 kg and a dwell time of 10 sec. A type 979 conductivity meter was used to measure the conductivity of alloys under various conditions. For these two measurements, 15 mm x 15 mm finished surfaces were created from all four alloys by grinding and polishing. Next, the conductivity data converted to electrical resistance to display it graphically.

The solutionized and 80 % deformed alloys were subjected to Differential scanning calorimetry where heating run in a Du Pont 900 instrument was used along with inert N_2 gas atmosphere. The DSC scan of a lump of 31.1 mg was conducted over a temperature range from 50°C to 400°C with the heating rate of 10°C min^{-1}. Nagasaki - Maesono analysis was employed to calculate the activation energy for transformations of different conditions [13]. XRD analyses of the cold rolled and one hour aged at 100°C alloys were carried out using a PANalytical Empyrean X-ray diffractometer with the Cu - Kα radiation and at a scanning rate of 1° min^{-1} and a Bragg angle 2θ ranging from 20° to 90°. Microstructures of the different possess samples were examined using Trinocular Inverted Metallurgical Microscope was of model SKU: ME1200TB-10MA. Additionally, the surface morphology of the cold-worked and aged samples was examined using a JEOL JSM-7600F model field emission scanning electron microscope. The EDX spectra of the samples were recorded using a JEOL EX - 37001 model electron dispersive spectrometer coupled with a FE - SEM setup. To observe the microstructure, the samples were finally polished with aluminium oxide and Keller's reagent was used as the etchant.

RESULTS AND DISCUSSION

Cold rolling

The variation of micro-hardness and electrical resistivity values with the different cold deformation of commercially pure Al, binary Al - Sn, Al - Pb and solder affected Al - Sn - Pb alloys are plotted in Fig. 1. It indicates that Sn and Pb addition improve the hardness of the cast alloys (Fig. 1a). It occurred due to the solute solution strengthening and their higher size of atoms than aluminium of the alloys [14]. However, Sn shows the superior hardness because of the dissimilar crystal orientation BCC of Sn precipitated within the FCC Al matrix whereas FCC Pb precipitates within FCC Al matrix. β - Sn precipitates might have generated coherency strain which leads to higher hardness in this alloy which probably is absent α - Pb precipitates in Al - Pb alloy. Consequently, the solder affected Al - Sn - Pb alloy displays the highest hardness. When the alloys are subjected to cold rolling higher hardness is achieved due to strain hardening. The reduction of rolling increases means plastically deformed more resulting in an increased dislocation density inside a material so makes more strengthen. Higher hardness values are obtained with small added alloys than pure aluminium because the elements create additional dislocations. The higher rate of hardness increases with cold rolling of Sn added alloy can be attributed to form the complex structure due to their different crystal structure than that of Al. This tendency also follows by the solder affected alloy [15].

Figure related the electrical resistivity, decreases gradually with the degree of deformation at the same background (Fig. 1b). Sometimes the cast alloys contents the porosity during casting. Porosity may reduce through the cold rolling results the decrease of electrical resistivity of alloys. When the deformation degree exits higher, it makes the material defect through higher

Table 1. Outlines the weight percent chemical composition of the alloys under investigation.

Alloy	Sn	Pb	Fe	Si	Cu	Mg	Mn	Ni	Zn	Cr	Ti	Al
Pure Al	0.002	0.002	0.202	0.280	0.008	0.014	0.048	0.008	0.036	0.001	0.002	Bal
Al - Sn	1.512	0.012	0.314	0.335	0.071	0.057	0.106	0.022	0.080	0.002	0.021	Bal
Al - Pb	0.002	1.275	0.335	0.345	0.069	0.055	0.111	0.010	0.075	0.003	0.021	Bal
Al - Sn - Pb	1.433	1.201	0.406	0.435	0.080	0.066	0.108	0.012	0.173	0.020	0.028	Bal

dislocation density. With the scale of cold processing, the electron scattering into the material increases, resulting in an increase in resistivity. This is due to distortion of the lattice structure or internal damage. Disc values are the result of two opposing effects. It appears that the first effect is greater than the second, and the electrical resistance decreases as a result. It also shows that the electrical resistance of pure aluminium is lower than that of alloys with the trace addition because the presence of other elements in the alloy always reduces electrical conductivity. Solid solution strengthening distorts the lattice, provides resistance to dislocation motion [16]. Again, Sn added alloy shows the higher resistivity because of its dissimilar crystal structure than Al and the same crystal structure of Pb added alloys shows the minimum and subsequently solder affected alloy displays the highest resistivity.

Thermal ageing

Isochronal ageing

Fig. 2 shows the changes in microhardness and electrical resistance of the alloys subjected to 80 % cold rolling, following an isochronally ageing treatment for a period of one hour. As the temperature rises to 100°C, alloys containing Sn and Pb exhibit some aging response followed by a profound decrease in hardness beyond 250°C (Fig. 2a). The age hardening results from the formation of various precipitates dispersed in the matrix. Aluminium does not form any intermetallic with neither Sn nor Pb as the solid solubility bound of Sn in Al is under 0.09 wt. % and Pb in Al is 0.2 wt. %. Even from the phase diagram, it can be confirmed and higher density difference among those is another reason for not formation of intermetallic [17, 18]. During casting alloys are accumulated some impurities from the environment. Whereas Sn tends to form various intermetallics with those impurities like Fe, Mg, Ni etc. But Pb does not have much tendency, consequently Sn has some aging response with higher intensity [19, 20]. Plastically deformed alloys usually have huge dislocations and put in more subgrains formation as affected by the grain orientation, which has an important role in the resulting high hardness. High temperature aging can be associated with stress relief, dislocation rearrangement, recovery, and grain growth of alloys. As recovery progresses, the deformed grains soften and the subgrains rotate and change to a new orientation. Recrystallization becomes more complete with aging at 350°C [21, 22].

Fig. 2b presents the results of electrical resistivity. It states that resistivity of alloy specimens at the early stage increases gradually at a certain point with the increase of ageing temperature. The conductivity of a material is proportional to the density of free electrons and the average free route of the electron, according to classical electronic theory, while the resistance of a material results from the collision of electrons with the lattice [23]. Early in the aging process, various intermetallics emerge, increasing the lattice distortion caused by impurity atoms, vacancies, internal dislocations, and external surfaces. These intermetallics also cause the

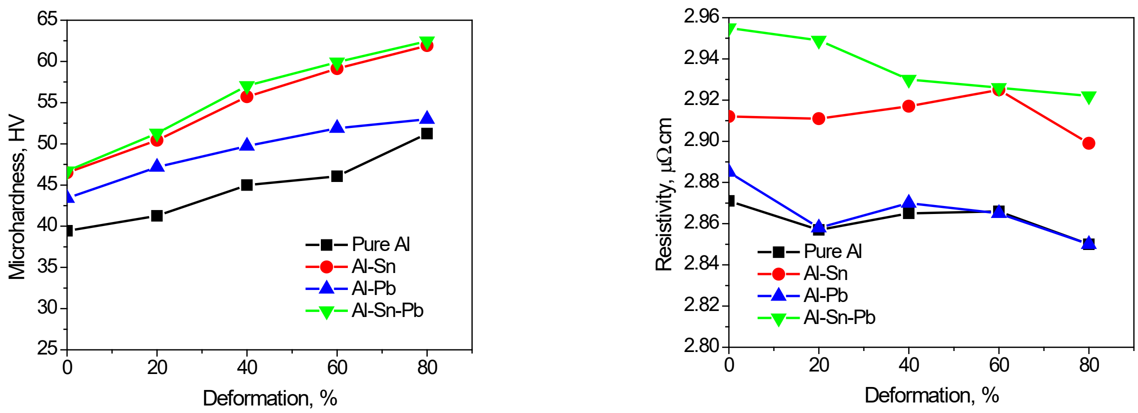

Fig. 1. (a) Micro-hardness and (b) Electrical resistivity values of the commercially pure Al, tin added Al - Sn, lead added Al - Pb and solder affected Al - Sn - Pb alloys under cold rolling by different percentages.

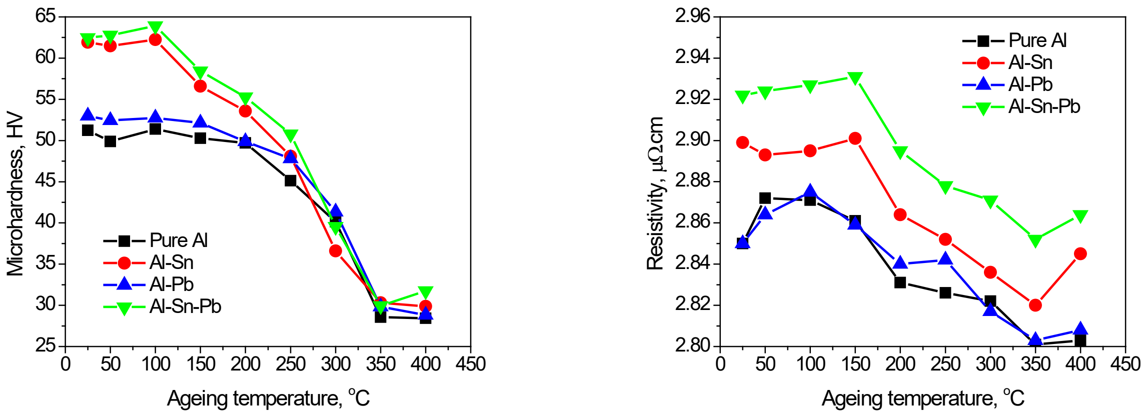

Fig. 2. Variation of (a) hardness and (b) resistivity due to the isochronally ageing of alloys for 1 h.

lattice's electric field to be non-uniform and intensify the scattering of electron waves, which raises the material's resistivity. Then, during a higher annealing procedure, both recovery and recrystallization took place. Recovery can lessen point defect concentration and grain flaws, which lessens the unevenness of the lattice's electric field. The electrical resistance is lowered as a result. Additionally, recrystallization can remove crystal grains and lattice deformation, eventually restoring the microstructure to its pre-cold rolling condition [21, 22]. Similar resistance levels of the alloys are shown, with the solder - affected alloy having the highest resistivity, followed by the alloy with Sn and Pb additions, and then pure Al as mentioned accessed previously.

Isothermal ageing

The effect of time - span of ageing at different temperatures like 50°C, 100°C and 150°C on the microhardness of 80 % cold rolled test alloys is shown in Figs. 3a - 3c. The results of the early isochronal aging of alloys, especially in the lower temperature range, are fully complying with this isothermal ageing response. All alloys exhibit an initial softening to dissolve the GP zone and relieve stress, followed by an increase in properties through the formation of intermetallic compounds. During the long aging process, softening occurs due to the recovery process of the alloy. At lower temperatures, this phenomenon disappears later. At higher aging temperatures, the dissolution of the GP zone, the formation of various metastable phases, and the recovery occur faster. This makes perfect sense given that as the temperature rises, the molecules gain energy and accelerate. Therefore, the likelihood of molecules moving with the activation energy needed to trigger the reaction during collisions increases as temperature rises. These figures show that the maximum hardness is achieved when the alloys are isothermally aged at 100°C for 60 min [21, 22].

Again, Fig. 4 presents the results of electrical resistivity of four alloys dependence of time under different ageing temperature. As a usual ageing at 50°C, 100°C and 150°C, due to precipitates formation through impurities, the resistivity of the alloys is increased initially and the resistivity decreases due to stress reliving as well as recovery (Figs. 4a - c). At the higher ageing temperate these occur earlier along with higher intensities for both faster intermetallic formation and recovery process. The individual level of electrical resistivity remains observed vales as explain earlier [21, 22].

DSC study

Directly cold - rolled by 80 % experimental alloys resulted in a DSC heating curve as shown in Fig. 5. All the alloys are attained an endothermic peak around 60°C, which are attributed for GP zones dissolution. It is already discussed that all the samples consist of different trace cast impurities with help to form the GP zones. The activation energy for the dissolution process of Al, Al - Sn, Al - Pb and Al - Sn - Pb alloys are 63, 64, 63 and 62 kJ mol^{-1} respectively as it is closed to the activation energy for dissolution of GP zone, 64.3 kJ mol^{-1} as reported

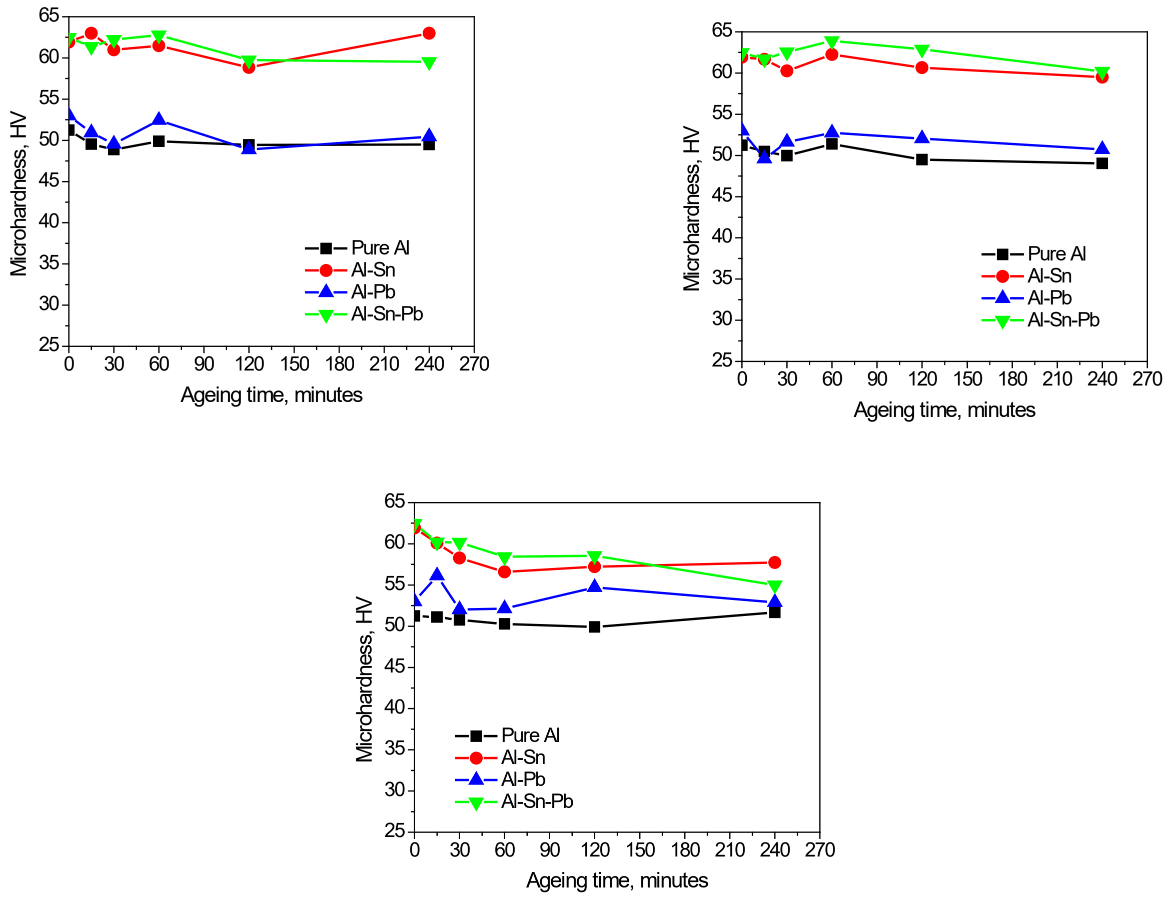

Fig. 3. Isothermal aging of 80 % cold - rolled experimental alloys at (a) 50°C, (b) 100°C, and (c) 150°C changes the microhardness with time.

earlier [24]. Tin added alloy shows an endothermic peak around 230°C. The activation energy of this process is close to that of tin diffusion, as reported in a previous study to be 62.3 kJ mol^{-1} [25, 26]. Similarly lead added alloy attains the endothermic peak around 327°C with an activation energy 87 kJ mol^{-1} for the diffusion of lead in aluminium where the activation energy has been reported to be 84.8 kJ mol^{-1} [27]. Whereas solder affected alloy displays two consecutive endothermic peaks around 182°C and around 212°C with the activation energy of 59.2 and 80.2 kJ mol^{-1} for dissolution of tin and lead respectively. More especially, it can be conveyed that the melting temperature of Sn is 232°C, Pb is 327.5°C and 60/40 Sn - Pb solder is 188°C.

XRD study

Fig. 6 shows the XRD patterns of four alloys at the condition of 80 % cold rolled and one-hour ageing at 100°C. Commercially pure Al shows the as usual peaks of Al [28]. But tin added alloy shows the additional peaks of Sn into the XRD pattern. Similarly, lead added alloys also displays the peaks associated with Pb. The solder affected alloy displays all the Al, Sn and Pb peaks into the XRD pattern. It is noted that except Al, the intensity of these elements is very low for their little amount presents into the Al - alloys. Additionally, there is no sign of any intermetallics in the XRD pattern as the trace amounts are relatively insignificant, which cannot be seen with the naked eye. This finding is also reported by earlier investigator [29].

Optical micrographs

Optical microstructures of commercially pure Al, binary Al - Sn, Al - Pb, and solder - affected Al - Sn - Pb alloys subjected to solution treatment and cold rolling by 80 % are shown in Figs. 7a - d. Equiaxed grains are

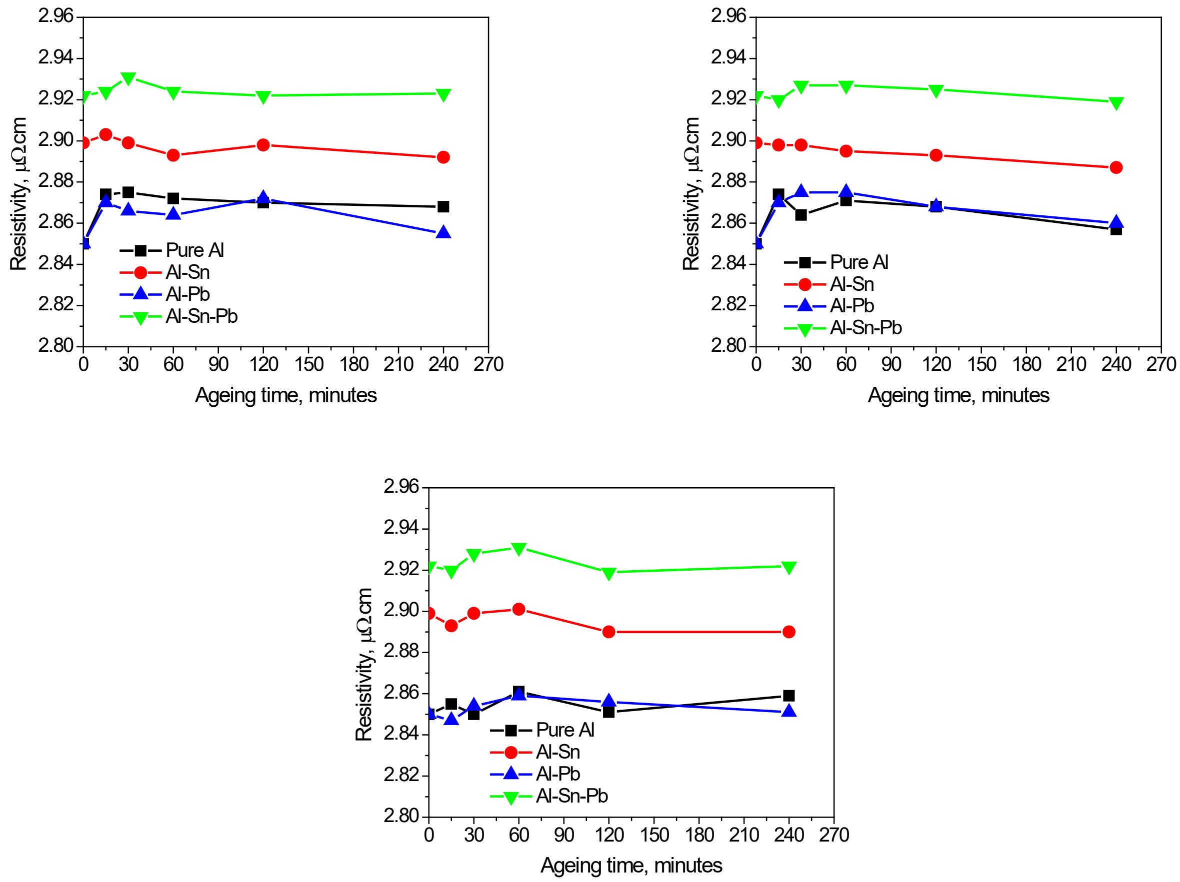

Fig. 4. Electrical resistance changes with time for isothermal aging of 80 % cold - rolled experimental alloys at (a) 50ºC (b) 100ºC and (c) 150ºC.

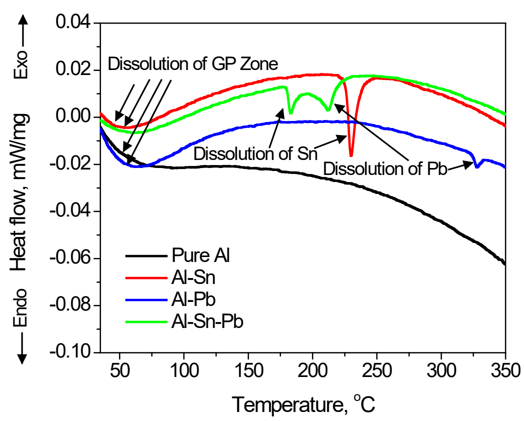

Fig. 5. DSC heating curve of experimental alloys.

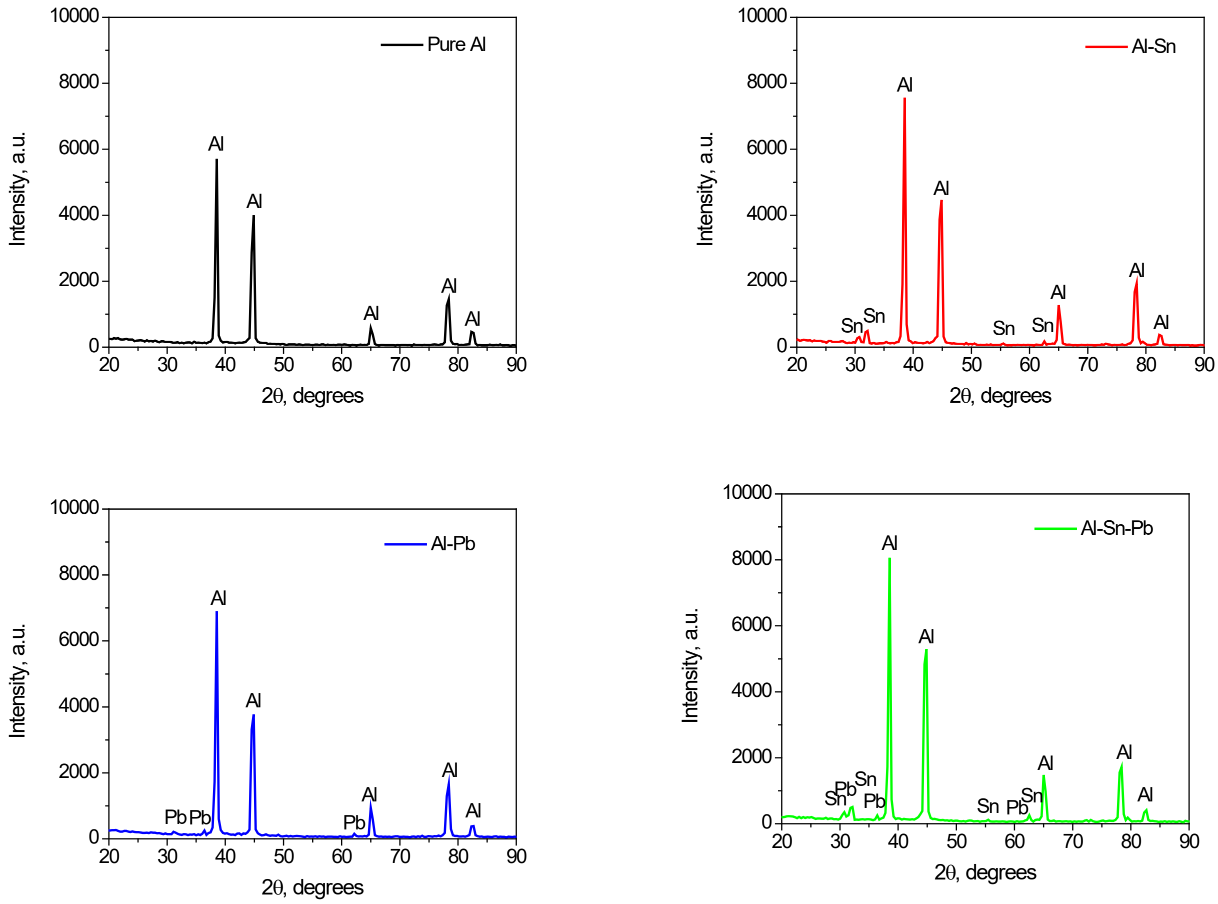

Fig. 6. The XRD patterns of the experimental Al and Al - alloys.

plastically deformed, which causes them to lengthen as they roll. The crystal grains become blurry due to the strong cold rolling, making it impossible to discern between them. Al's microstructure is made up mostly of α - Al and a few minor impurities that are dispersed along the grain boundaries. Primary aluminium, β - tin, and trace intermetallic make up the Sn added alloy. Because BCC β - tin stays at the grain boundary, the grain boundary is quite thick. In line with this, the microstructure of the alloy with Pb added is composed mostly of aluminium, lead, and trace impurities. For the identical FCC crystal structure of α - lead and Al, the grain boundary is relatively not as thick as the alloy added with tin. The alloy affected by solder demonstrates how both constituents have an influence on its microstructure [30, 31].

Related alloys achieved the equiaxed grain structure during the ageing process at 350°C for 1h. Fig. 8a - d shows the revealed microstructures under such heat treatment regime. The long grains are not present. All the lead, tin, and trace intermetallic phases dissolve into the grain boundaries and matrix of aluminium. As a result, the grain boundary no longer just becomes apparent, but also bushy. Contrarily, traces of indissoluble phases of Fe and Si may still be seen at the edges of grains as well as within them [30]. In addition, solder - influenced alloys have a larger proportion of dissolved second phase in the microstructure, ensuring thicker grain boundaries.

SEM observation

Solution treated and cold rolled by 80 % and then aged at 100°C for 1 h, the SEM images along with EDX spectra of commercially pure Al, binary Al - Sn, Al - Pb and solder affected Al - Sn - Pb alloys are shown in Figs. 9a - d. Between the microstructure there are not enough differences are observed as the level of doped

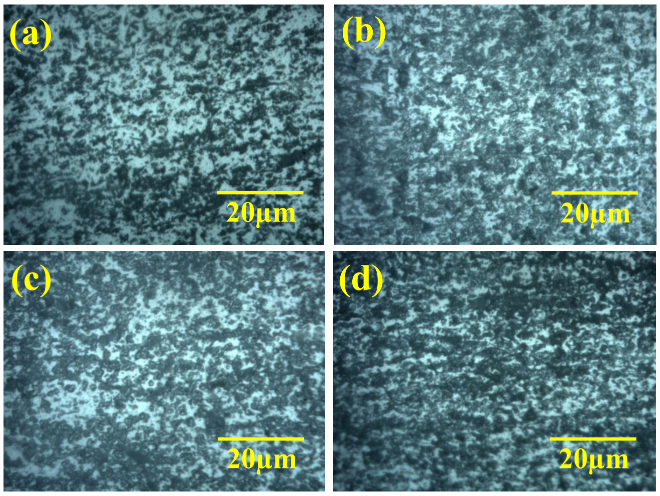

Fig. 7. Optical micrograph of 80 % cold rolled (a) commercially pure Al, (b) tin added Al - Sn, (c) lead added Al - Pb and (d) solder affected Al - Sn - Pb alloys.

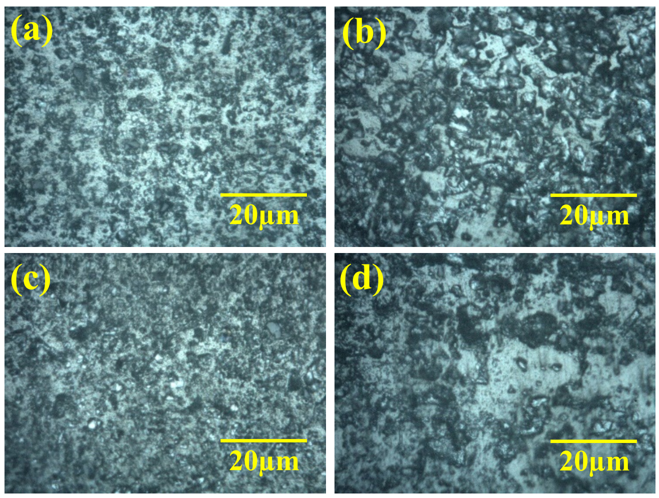

Fig. 8. Optical micrograph of experimental alloys after ageing at 350°C for 1h (a) Al, (b) Al - Sn, (c) Al - Pb and (d) Al - Sn - Pb alloys.

elements Sn and Pb are small, additionally they do not form intermetallics with Al. Some cases the elements added alloys show the higher size particles as well as the higher dense of particles size in the background of the microstructure. Due to plastic deformation, equiaxed grains elongate regularly in the rolling direction. For severe deformation, the crystal grains become blurred, and the crystal grains are difficult to distinguish. Ageing at this temperature generally does not change the grain orientation of Al alloys [30]. Some stress reliving may occur with the formation of GP zones. Thus, the microstructure of pure Al consists of the solid phases of α - Al and various intermetallic produced by trace impurities. The alloy microstructure of tin is composed of primary aluminium, β - tin and various impurity intermetallic. Since it has the BCC crystal structure which is different from FCC of Al, it tends to distribute at grain boundaries resulting in dense grain boundaries. Similarly, alloy containing lead shows primary aluminium, α - lead and impurities distributed in the microstructure. But grain boundaries are not very thick because both Pb and Al alloys have the FCC crystal structure. The solder affected alloy reflects the addition of both elements [31]. The corresponding EDX of the SEM of Al reveals the following chemical composition by the weight percentage as 99.18 % Al, 0.19 % Si,

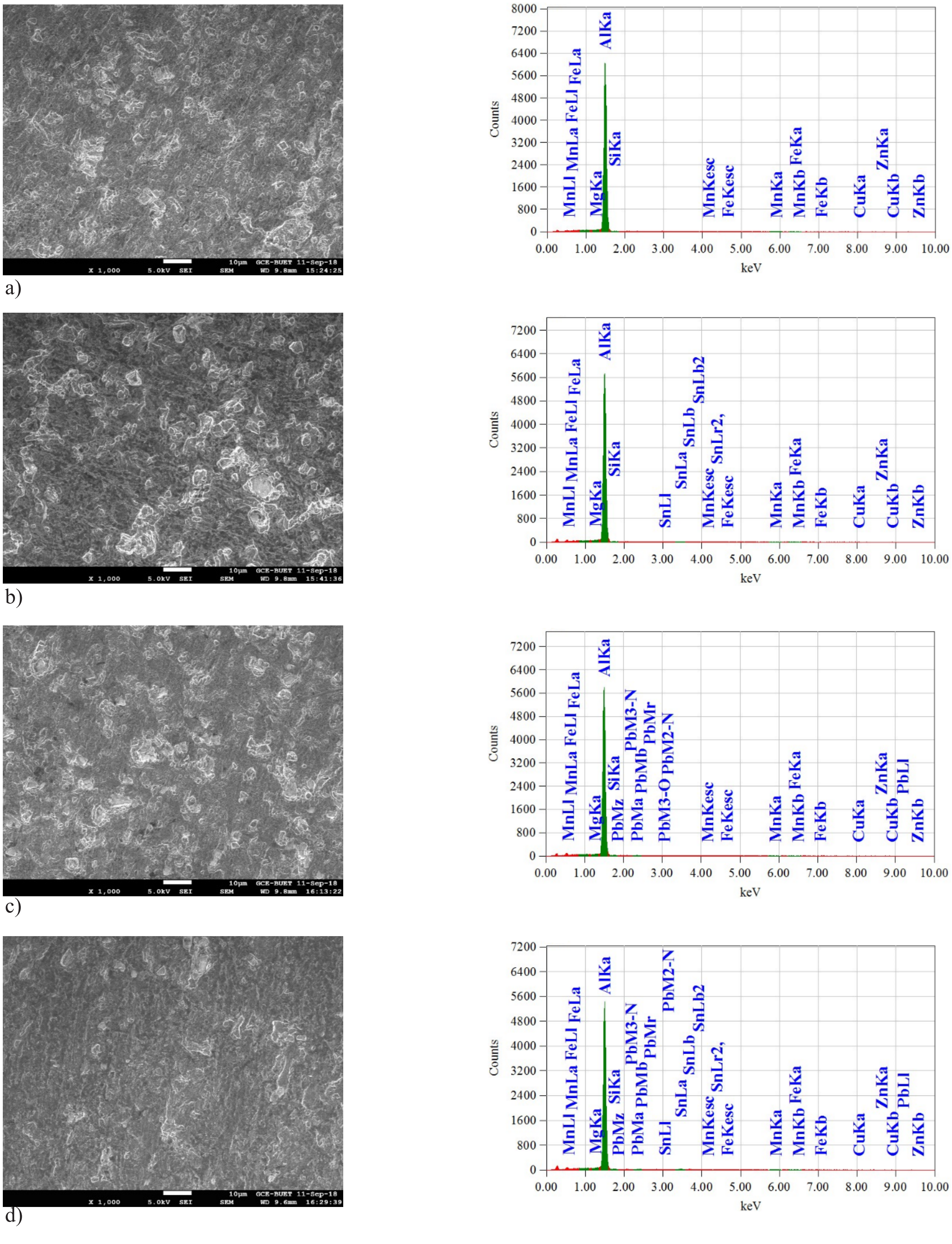

Fig. 9. SEM images and EDX spectra of the cold rolled and aged (a) commercially pure Al, (b) binary Al - Sn, (c) Al - Pb and (d) solder affected Al - Sn - Pb alloys.

0.24 % Cu and 0.39 % Zn. The EDX scan reveals the following chemical composition by weight percentage of Al - Sn Alloy as 99.22 % Al, 0.41 % Si, 0.08 % Mn and 1.29 % Sn. Similarly, Al - Pb alloy shows 98.33 % Al, 0.42 % Si, 0.05% Mn, 0.08% Cu, 0.12 % Zn and 1.01 % Pb. The solder affected Al - Sn - Pb alloy consists of 92.90 % Al, 0.66 % Si, 0.34 % Mn, 0.08 % Mg, 4.18 % Sn and 1.84 % Pb.

CONCLUSIONS

The effect of solder on the different properties and microstructure changes of pure aluminium system were surveyed and the main results are:

Solder has a positive effect on hardness of pure Al due to solid solution strengthening. Aluminium has FCC crystal structure, but Sn is the BCC structure so higher incoherency gives better results compared to the FCC crystal structure of Pb. This is why electrical resistivity also increases of the element added alloys and the Sn has the higher effect on the property. During aging, since both Sn and Pb do not form any intermetallics with Al, but in most cases, Sn forms different intermetallics with cast impurities than Pb consequently Sn gives a higher aging effect and Solder affected alloy exhibits additive age hardening effects especially at low ageing temperature. At higher ageing temperature there is no benefit as it recrystallized earlier for desolation at low temperature. Due to the formation of fine precipitates electrical resistivity increased, but at higher ageing temperature it decreases due to precipitate coarsening as well as recovery and recrystallization. Tin and lead do not form any intermetallics with Al but DSC and XRD study confirms the presence of those elements into alloys. Equiaxed grains are elongated in the rolling direction due to plastic deformation. The intense cold rolling causes the crystal grains to blur, making them difficult to distinguish. All alloys have reached a fully recrystallized state after annealing at 350°C for one hour but the solder affected alloys demonstrates the higher fraction of the dissolved second phase in the microstructure and demonstrates developed grain boundaries.

Acknowledgements

The Miyan Research Institute of International University of Business Agriculture and Technology, Dhaka is acknowledged for providing financial support to carry out the project work. The author would like to express his appreciation to the Director of Administration, Prof. Selina Nargis for all of the helpful support and encouragement she has made available in advancing research activities at the university.

Authors' contributions: The complete dedication and active participation displayed in all stages of the paper, inculding comming up with ideas, developing the methodology, drafting the content, conducting reviews, and making edits, should be credited to M.K.

REFERENCES

1. M. Tehrani, Advanced Electrical Conductors: An Overview and Prospects of Metal Nanocomposite and Nanocarbon Based Conductors, Phys. Status Solidi., 218, 8, 2021, 1-17.
2. ASM Handbook Committee. Properties and Selection: Nonferrous Alloys and Special-Purpose Materials, ASM International, 2, Materials Park, Ohio, USA, 1990.
3. A. Das, A. Barai, I. Masters, D. Williams, Comparison of Tab-To-Busbar Ultrasonic Joints for Electric Vehicle Li-Ion Battery Applications, World Electr. Veh. J., 10, 3, 2019, 1-11.
4. V. Sivasubramaniyam, S. Ramasamy, M. Venkatraman, G. Gatto, A. Kumar, Carbon Nanotubes as an Alternative to Copper Wires in Electrical Machines: A Review, Energies, 16, 9, 2023, 1-17.
5. Q. Guan, C. Hang, S. Li, D. Yu, Y. Ding, X. Wang, Y. Tian, Research progress on the solder joint reliability of electronics using in deep space exploration, Chin. J. Mech. Eng., 36, 22, 2023, 1-13.
6. V.K. Soo, J. Peeters, D. Paraskevas, P. Compston, M. Doolan, J.R. Duflou, Sustainable aluminium recycling of end-of-life products: A joining techniques perspective, J. Clean. Prod., 178, 2018, 119-132.
7. M.E. Mehtedi, P. Buonadonna, M. Carta, R.E. Mohtadi, A. Mele, D. Morea, Sustainability Study of a New Solid-State Aluminum Chips Recycling Process: A Life Cycle Assessment Approach, Sustainability, 15, 2023, 1-14.
8. R. Branco, F. Berto, A. Kotousov, Special Issue on "Mechanical Behaviour of Aluminium Alloys", Appl.

Sci., 2018, 8, 1-3.
9. M.S. Kaiser, S. Datta, A. Roychowdhury, M.K. Banerjee, Age Hardening Behavior of Wrought Al-Mg-Sc Alloy, Mater. Manuf. Process., 23, 1, 2007, 74-81.
10. C.H. Ng, S.N.M. Yahaya, A.A.A. Majid, Reviews on aluminum alloy series and its applications, Acad. J. Sci. Res., 5, 12, 2017, 708-716.
11. M.A. Nur, A.A. Khan, S.D. Sharma, M.S. Kaiser, Electrochemical corrosion performance of Si doped Al-based automotive alloy in 0.1 M NaCl solution, J. Electrochem. Sci. Eng., 12, 3, 2022, 565-576.
12. Y. Chen, H. Yu, Y. Chen, H. Di, W. Xu, The strengthening effects and mechanisms of alloying elements on interfaces for multiphase Ni-based superalloys: A first-principles study, J. Mater. Res. Technol., 23, 2023, 4802-4813.
13. S. Nagasaki, A. Maesono, High Temperatures – High Pressures (HTHP), F. Met. Phys., 11, 1965, 182-188.
14. E.W. Collings, H.L.Gegel, Physical Principles of Solid Solution Strengthening in Alloys, Springer, Boston, USA, 1975.
15. K.I. Elkhodary, M.A. Zikry, Dynamic crack nucleation, propagation, and interactions with crystalline secondary phases in aluminum alloys subjected to large deformations, Philos Mag., 92, 32, 2012, 3920-3949.
16. S. Nestorovic, D. Markovic, L. Ivanic, Influence of degree of deformation in rolling on anneal hardening effect of a cast copper alloy, Bull. Mater. Sci., 26, 6, 2003, 601-604.
17. A.J. McAlister, The Al-Pb (Aluminum-Lead) system, Bull. Alloy Phase Diagr., 5, 1984, 69-73.
18. A.J. McAlister, D.J. Kahan, The Al-Sn (Aluminum-Tin) System Bull. Alloy Phase Diagr., 4, 1983, 410-414.
19. M.S. Kaiser, Tensile and Fracture Behaviour of Sn/Pb Solder Affected Aluminium Subjected to Post-Deformation Ageing, IUBAT Review, 7, 1, 2024, 186-201.
20. B. Schwager, M. Ross, S. Japel, R. Boehler, Melting of Sn at high pressure: Comparisons with Pb, The Journal of Chemical Physics, 133, 084501, 1-3.
21. M.S. Kaiser, Trace impurity effect on the precipitation behaviour of commercially pure aluminium through repeated melting, Eur. J. Mater. Sci. Eng., 5, 1, 2020, 37-48.
22. S. Nestorovic, Influence of alloying and secondary annealing on anneal hardening effect at sintered copper alloys, Bull. Mater. Sci., 28, 5, 2005, 401-403.
23. V. Palenskis, Free Electron Characteristic Peculiarities Caused by Lattice Vibrations in Metals, J. Condens. Matter. Phys., 12, 2, 2022, 9-17.
24. Y. Ma, Y. Huang, X. Zhang, Precipitation thermodynamics and kinetics of the second phase of Al-Zn-Mg-Cu-Sc-Zr-Ti aluminum alloy, J. Mater. Res. Technol., 10, 2021, 445-452.
25. M.D. Mathew, H. Yang, S. Movva, K.L. Murty, Creep deformation characteristics of tin and tin-based electronic solder alloys, Metall. Mater. Trans. A., 36, 2005, 99-105.
26. Y. Liu, W. Yu, Y. Liu, Effect of ultrasound on dissolution of Al in Sn, Ultrason Sonochem, 50, 2019, 67-73.
27. W. Zhifang, L. Chao, W. Run, C. Qingming, Coarsening Kinetics of Pb Phase in a Nanocomposite Alloy Produced by Mechanical Alloying in Immiscible Al-Pb System and the Influence of Cu Addition on It, Rare Metal. Mat. Eng., 46, 12, 2017, 3675-3681.
28. X. Xu, Z. Liu,B. Zhang,H. Chen, J. Zhang, T. Wang, K. Zhang, J. Zhang, P. Huang, Effect of Mn content on microstructure and properties of 6000 series aluminum alloy, Appl. Phys. A., 2019, 125, 490, 1-9.
29. C.A. Billur, M. Ari, T. Karaaslan, B. Saatci, Structural, electrical, thermal, mechanical properties and micro-hardness in Sn-based Sn-Pb-Al ternary alloys, Cumhuriyet Sci. J., 8, 4, 2017, 39-51.
30. M.S. Kaiser, Fractional recrystallization behavior of impurity-doped commercially pure aluminium, J. Energy Mechanical Material Manufacturing Eng., 5, 2, 2020, 37-46.
31. C.A. Billur, E. Gerçekcioglu, M. Bozoklu, B. Saatçi, M. Ari, F. Nair, The electrical, thermal conductivity, microstructure and mechanical properties of Al-Sn-Pb ternary alloys, Solid State Sci., 46, 2015, 107-115.